

Amorphous Molecular Materials for Directed Supercontinuum Generation

Stefanie Dehnen,^{*,[a, h]} Peter R. Schreiner,^{*,[b, i]} Sangam Chatterjee,^[c, i] Kerstin Volz,^[d, h]
Nils W. Rosemann,^[e] Wolf-Christian Pilgrim,^[a, h] Doreen Mollenhauer,^[f, i] and Simone Sanna^[g, i]

Molecular compounds of the general formula $[(RT)_4E_6]$ (R = organic or organometallic substituent; T = C, Si, Ge, Sn; E = CH₂, S, Se), hence adamantane derivatives and inorganic-organic hybrid compounds based on a heteroadamantane structure exhibit a non-linear optical response upon radiation with a continuous-wave near-infrared laser. The effect depends on the compounds' habitus, which itself depends on the elemental composition of the cluster core, and on the nature of the organic substituents. A combination of these parameters that cause the material to be intrinsically amorphous leads to

supercontinuum generation and thus to the emission of a broad spectrum, potentially appearing as white light. Notably, the emission essentially retains the driving laser's directionality. For crystalline samples, second harmonic generation is observed instead, which points to a close relationship of the optical properties and the intermolecular order. Variation of R, T, and E allows further fine-tuning of the emitted spectra. We present all studies made in regards to these effects and our overarching conclusions derived from them.

1. Introduction

The development of new, efficient, and sustainable light sources for a variety of applications is an ongoing process, in which the light emitting or light converting materials range from classic inorganic phosphors and semiconductors^[1,2] for LED applications and their organic equivalents^[3,4] to a plethora of different molecular phosphors.

Among the light generation processes, white-light generation (WLG) is one of the most puzzling and exciting topics in nonlinear optics. WLG is the common denomination of a physical phenomenon referred to as supercontinuum generation, i.e., the extreme spectral broadening of a light source propagating through a nonlinear medium.^[5,6] From a physical point of view, supercontinuum generation is the combined effect of a multitude of nonlinear optical mechanisms (ranging from self-/cross-phase modulation and four-wave mixing to solitonic phenomena), which sum up to extremely broad spectra resembling white light. WLG upon irradiation of a material with near-infrared continuous-wave (NIR CW) lasers has been observed in (doped) oxides, oxidic hybrid compounds, rare earth-based complexes, and carbon-based materials.^[7] The reasons for WLG to occur can vary from case to case, which demands a closer look at every individual single compound class. In this minireview, we shed light on amorphous molecular materials based on (hetero)adamantane-type molecules, which have recently been shown to be able to generate a supercontinuum. In particular, we explore the relationships between chemical composition, atomic and electronic structure, and optical response to determine the prerequisites for WLG.^[8-13]

Heteroadamantane clusters with organic substituents of the type $[(RT)_4E_6]$ (R = organic or metalorganic substituent; T = Si, Ge, Sn; E = S, Se, Te^[14]) and derivatives of organic adamantane

[a] Prof. Dr. S. Dehnen, Prof. Dr. W.-C. Pilgrim

Department of Chemistry
Philipps University Marburg
Hans-Meerwein Straße 4, 35043 Marburg (Germany)
E-mail: dehnen@chemie-uni-marburg.de

[b] Prof. Dr. P. R. Schreiner

Institute of Organic Chemistry
Justus Liebig University Giessen
Heinrich-Buff-Ring 17, 35392 Giessen (Germany)
E-mail: prs@uni-giessen.de

[c] Prof. Dr. S. Chatterjee

Institute of Experimental Physics I
Justus Liebig University Giessen
Heinrich-Buff-Ring 17, 35392 Giessen (Germany)

[d] Prof. Dr. K. Volz

Department of Physics
Philipps University Marburg
Renthof 5, 35032 Marburg (Germany)

[e] Dr. N. W. Rosemann

Light Technology Institute
Karlsruhe Institute of Technology
Engesserstrasse 13, 76131 Karlsruhe (Germany)

[f] Prof. Dr. D. Mollenhauer

Institute of Physical Chemistry
Justus Liebig University Giessen
Heinrich-Buff-Ring 17, 35392 Giessen (Germany)

[g] Prof. Dr. S. Sanna

Institute of Theoretical Physics
Justus Liebig University Giessen
Heinrich-Buff-Ring 16, 35392 Giessen (Germany)

[h] Prof. Dr. S. Dehnen, Prof. Dr. K. Volz, Prof. Dr. W.-C. Pilgrim

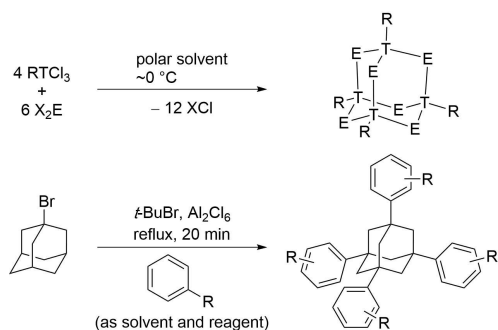
Materials Science Center (WZMW)
Structure and Technology Laboratory (STRL)
Hans-Meerwein Straße 6, 35043 Marburg (Germany)

[i] Prof. Dr. P. R. Schreiner, Prof. Dr. S. Chatterjee, Prof. Dr. D. Mollenhauer,

Prof. Dr. S. Sanna
Center for Materials Research (ZfM)
Justus Liebig University Giessen
Heinrich-Buff-Ring 16, 35392 Giessen (Germany)

© 2021 The Authors. ChemPhotoChem published by Wiley-VCH GmbH. This is an open access article under the terms of the Creative Commons Attribution License, which permits use, distribution and reproduction in any medium, provided the original work is properly cited.

derivatives, $(\text{CR})_4(\text{CH}_2)_6$, have been investigated with respect to their synthesis and structures for quite some time, and many examples with differing elemental compositions^[15–21] and a variety of ligands^[22–26] were realized. Note that besides these “regular” adamantane cages, various mixed versions have been known, in which more than one T, R, or E are present in one molecule – including inorganic-organic hybrid cages – which can be accessed by various synthetic approaches.^[27–31] However, as such compounds (with one exception, see below) have not yet been investigated with respect to their optical properties, we are not going to elaborate on them here. The most straightforward access to heteroadamantane-based clusters $[(\text{RT})_4\text{E}_6]$ is realized by condensation reactions between a chalcogenide source X_2E ($\text{X} = \text{Na}, \text{SiMe}_3$) and an organotetrel trichloride RTCl_3 . The organic counterpart, hence derivatives of adamantane, can be accessed through Friedel-Crafts reactions of 1-bromoadamantane in slurries of *t*-butyl bromide and



Scheme 1. Top: General reaction scheme for the synthesis of heteroadamantane clusters of the general formula $[(\text{RT})_4\text{E}_6]$ with chalcogen sources X_2E ($\text{R} = \text{organic or organometallic substituent}; \text{T} = \text{Si, Ge, Sn}; \text{E} = \text{S, Se, Te}; \text{X} = \text{alkali metal ion, SiMe}_3$). Bottom: Synthesis scheme for purely organic adamantane derivatives.

aluminum chloride using the aryl component as solvent.^[32] Both general syntheses are illustrated in Scheme 1.

In contrast to the isomeric “double-decker”-type structure of $[(\text{RT})_4\text{E}_6]$, which is obtained in the presence of ligands like $\text{R} = \text{CMe}_2\text{CH}_2\text{C}(\text{O})\text{Me}$ that allow for $\text{O} \cdots \text{T}$ back-coordination,^[33] the adamantane-type architecture does not possess inversion symmetry.^[34] Hence, these compounds, as well as their organic counterparts, were investigated with respect to non-linear optical properties. After irradiation with an inexpensive NIR CW laser diode, they either exhibit WLG or strong second harmonic generation (SHG), depending upon the nature of the substituent R and the intermolecular order in the solid state resulting from it.

Here, we will give a chronological overview of the research done in this specific area of WLG and SHG generation with the compounds under consideration. This includes the syntheses and crystal structure determinations, the investigation of linear and nonlinear optical absorption properties, exploration of morphology and molecular aggregation in amorphous samples, and quantum chemical investigations of geometric and electronic structures of the clusters as well as solid materials based on them. All compounds studied and reported so far are summarized in Table 1, along with a brief comment on their respective morphology and optical response. From the observations so far, it is possible to draw some conclusions, but the overall message is that the detailed understanding of the excitation and emission pathways is still to be unraveled. At the end of this article, we will summarize the knowledge gathered so far and propose an outline of the current ideas.

Table 1. Adamantane-like and adamantane-based compounds investigated to date in regard of their non-linear optical response to NIR CW laser irradiation. The colored line in the leftmost column indicates the color code used in the figures to indicate the respective compound.

Compound	Habitus ^[a]	Optical response	Remarks
$[(\text{StySn})_4\text{S}_6]$ (1) ^[8]	—	a	WLG Sty = styryl
$[(\text{PhSn})_4\text{S}_6]$ (2) ^[12]	—	a	WLG
$[(\text{MeSn})_4\text{S}_6]$ (3) ^[12]	—	a	SHG
$[(\text{NpSn})_4\text{S}_6]$ (4) ^[12]	—	a	SHG
$[(\text{BnSn})_4\text{S}_6]$ (5) ^[10]	—	c	SHG
$[(\text{R}^1\text{Sn})_4\text{S}_6]$ (6) ^[10]	—	a	WLG $\text{R}^1 = (\text{CH}_2)_2 - (\text{C}_6\text{H}_4)\text{CO}_2\text{Et}$
$[(\eta^1\text{-CpSn})_4\text{S}_6]$ (7) ^[10]	—	a	WLG
$[(\text{CySn})_4\text{S}_6]$ (8) ^[10]	—	a	WLG
$[(\text{PhSn})_4\text{Se}_6]$ (9) ^[10]	—	a	WLG
$[(\text{BnSn})_4\text{Se}_6]$ (10) ^[10]	—	c	WLG Melts upon irradiation
$[(\text{R}^1\text{Sn})_4\text{Se}_6]$ (11) ^[10]	—	a	WLG $\text{R}^1 = (\text{CH}_2)_2 - (\text{C}_6\text{H}_4)\text{CO}_2\text{Et}$
$[(\eta^1\text{-CpSn})_4\text{Se}_6]$ (12) ^[10]	—	a	WLG
$[(\text{CySn})_4\text{Se}_6]$ (13) ^[10]	—	a	WLG
$[(\text{PhGe})_4\text{S}_6]$ (14) ^[12]	—	a	WLG
$[(\text{PhSi})_4\text{S}_6]$ (15) ^[9]	—	c	SHG
$[(\text{NpSi})_4\text{S}_6]$ (16) ^[9]	—	c	None
1,3,5,7-Tetraphenyl-adamantane (17) ^[13]	—	a	WLG Nearly insoluble material ^[34]
	—	c	SHG
$[(\text{Me}_3\text{P})_3\text{AuSn}\{\text{PhSn}\}_3\text{S}_6]$ (18) ^[11]	—	c	WLG Amorphization upon laser irradiation
$[(\text{Et}_3\text{P})_3\text{AgSn}\{\text{PhSn}\}_3\text{S}_6]$ (19) ^[11]	—	c	WLG Amorphization upon laser irradiation
$[(\text{Me}_3\text{P})_3\text{CuSn}\{\text{PhSn}\}_3\text{S}_6]$ (20) ^[11]	—	c	None WLG hindered by re-absorption

[a] a = amorphous, c = (single-)crystalline.

2. Materials Investigations

The first studies about WLG in adamantane like compounds were carried out on [(StySn)₄S₆] (**1**, Sty = styryl), which serves as the archetypal compound for this effect. The goal was to produce an amorphous compound combining inorganic semiconductor materials with organic substituents containing delocalized π -electrons from readily available materials. As the formation of crystals of **1** was unsuccessful, the heteroadamantane structure was verified indirectly by means of NMR spectroscopy, mass spectrometry, and quantum chemical computations using density functional theory (DFT; Figure 1a). An NIR CW laser diode was used to study the emission properties of the amorphous solid, which turned out to emit warm white light, with a color impression close to that of a tungsten halogen bulb. Notably, the effect was obtained with an inexpensive diode, and not with a pulsed laser, which has been used for WLG since the 1970s. Even more noteworthy is, however, that the emitted light shows high brilliance and widely retains the directionality of the driving laser, thus resulting in a low etendue (Figure 1f).

The WLG output power scales to about the power of eight in relation to the pump-power density, demonstrating the

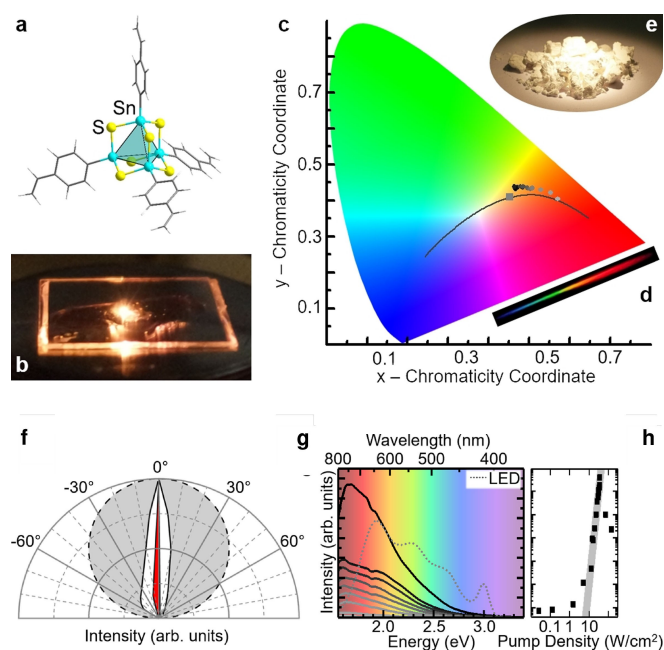


Figure 1. a: Molecular model of **1** from DFT computations. b: Photograph of **1** in a polymer film sandwiched between two glass plates excited by an 800 nm laser. c: Color temperatures given for excitation fluencies, indicated by gray scale data points next to ideal black body emission at varying temperatures (gray line) and the color temperature of a standard emitter at 2856 K (square). d: Photograph of the dispersed white-light spectrum. e: Photograph of the as-prepared powder. f: Highly directional spatial emission pattern of the white-light spectrum emitted by **1** (white) and the CW excitation laser at 980 nm (red) compared to a perfect Lambertian emitter (gray). g: Spectra of the white light emission of **1** after excitation with a 980 nm (1.265 eV) laser at varying powers from 6 mW (light gray solid line) to 18 mW (black solid line). For comparison, the normalized spectra of the white-light of a GaN-based LED (dotted) is given. h: Double-logarithmic plot of the white light input-output characteristics. Adapted with permission from Ref. [8]. Copyright (2016) AAAS.

extreme nonlinearity of this effect. Lower pump power leads to the peak maximum shifting to lower energies. For more detailed insights, the absorption spectrum and a spectrum of the above-bandgap UV-laser driven spontaneous emission were also recorded. In accordance with the Franck-Condon principle, both spectra are mirror images of each other. Compared to infrared-driven WLG, the spontaneous emission produces a narrower spectrum, which in addition is shifted to higher energies and appears with significantly lower intensity. Another notable difference is found in the lifetime of both effects after pulse excitation. While the spontaneous emission decays after several 100 ps, WLG shows a lifetime beyond the instrument-limited 10 μ s mark. This excludes conventional coherent processes as a mechanism for the NIR-driven WLG and indicates that the directionality is caused by a phased-array effect induced by the continuously present electric field of the driving CW laser.

With regard to the potential use of corresponding white-light emitters, the deposition on semiconductor surfaces was tested and proven possible by sublimation of compound **1** onto H-terminated Si(001) and GaAs(001) surfaces and subsequent investigation by means of energy-dispersive X-ray (EDX) spectroscopy and high-angle annular dark-field scanning transmission electron microscopy (HAADF-STEM) analyses of the resulting monolayer (Figure 2). The image shows long-range homogeneity, but also reveals the lack of long-range order. Thus, also a monolayer of **1** was found to be amorphous.

Encouraged by the properties detected for the archetypal compound **1**, the investigations were extended to other heteroadamantane-based compounds, in which the organic substituent as well as the elemental composition of the cluster core were varied. The study included the simple and long-known compound [(PhSn)₄S₆] (**2**), as it also features intrinsic amorphousness as well as delocalized π -electrons in the organic substituent; furthermore, its synthesis is even simpler than that of **1**. WLG was observed for **2**, with only minor shifts of the emitted spectrum when compared to **1**. This finding rendered **2** an ideal benchmark compound for further investigations.

Due to missing long-range order, the molecular structure of **2** could not be elucidated by conventional X-ray diffraction. Instead, the absolute static structure factor $S(Q)$ had to be

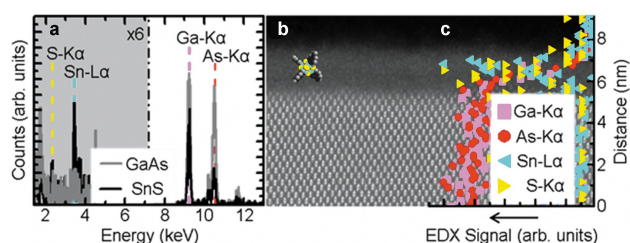


Figure 2. a: EDX spectra revealing the contributions of Sn and S in the amorphous cluster layer and Ga and As in the crystalline substrate. b: The self-assembled monolayer, with a scaled structure model overlaid on the micrograph to illustrate the size. c: EDX line scans indicating the distribution of the elements in the sample shown in the micrograph. Reproduced with permission from Ref. [8]. Copyright (2016) AAAS.

determined by means of total synchrotron scattering. The desired structural real-space information was then obtained from molecular Reverse-Monte-Carlo (RMC) simulations.^[35–37] For this, rigid model molecules of **1** and **2** were used, whose structural parameters were previously obtained from DFT calculations.^[8,12] A total of 216 molecules were moved inside a virtual simulation box along their rotational and translational degrees of freedom. In each step, the theoretical structure factor was calculated from the simulated atomic positions until best possible agreement between the experimental and the calculated $S(Q)$ was achieved.^[38,39]

This way it was possible to confirm the adamantane-type structure of **1** as opposed to the isomeric “double-decker”-type structure. This is depicted in Figure 3, where the full red and the dashed blue lines represent RMC-simulation results of the

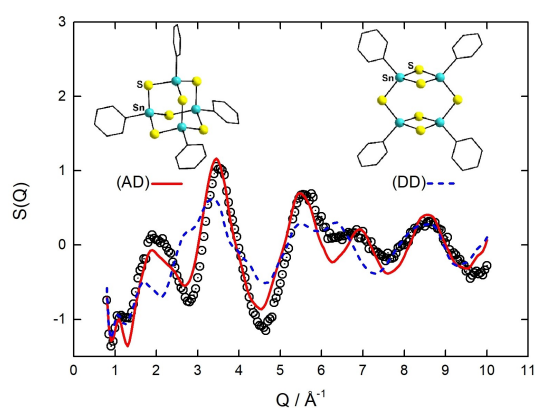


Figure 3. Experimental structure factors of compound **2** (circles) compared to the best fit of Reverse-Monte-Carlo (RMC) simulations of the two proposed structural models of **2**, the adamantane type (AD, red solid line) and the double-decker type (DD, blue dashed line), illustrated as calculated structures. Reproduced under terms of the CC-BY license.^[39] Copyright 2020, The Authors, Published by IOP Publishing.

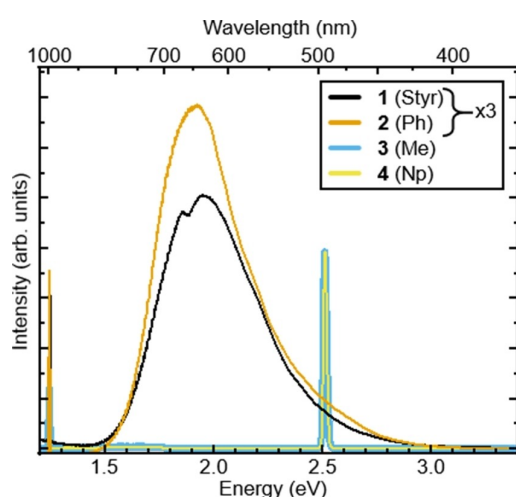


Figure 4. Emission spectra of amorphous samples of **1**, **2**, **3**, and **4** after excitation with a 980 nm (1.265 eV) laser. **1** and **2** show WLG, while **3** and **4** show SHG (2.53 eV). Reproduced with permission from Ref. [12]. Copyright (2016) ACS.

adamantane-type **1** and the “double-decker”-type **2**, respectively. Circles give the experimental $S(Q)$.

A more drastic change was introduced to the organic substituents by attachment of methyl or naphthyl groups to the tin atoms, yielding $[(\text{MeSn})_4\text{S}_6]$ (**3**) or $[(\text{NpSn})_4\text{S}_6]$ (**4**). Both compounds showed SHG (Figure 4), although powder X-ray diffraction (PXRD) experiments did not indicate crystalline long-range order. This observation was explained with the lack of π -electrons in the case of **3**, but required another rationale for compound **4**. Here, the most plausible conclusion so far is that the naphthyl groups may cause π -stacking interactions that allow for a certain degree of intermolecular interactions with short to medium range spatial extension. Obviously, this already prohibits WLG, which seems to require an even lower degree of order.

To specifically investigate the role of the π -electrons regarding their position, delocalization, and general presence in the organic substituent, the following series of compounds was synthesized and their potential for WLG was investigated, $[(\text{BnSn})_4\text{S}_6]$ (**5**; Bn = benzyl), $[(\text{R}^1\text{Sn})_4\text{S}_6]$ (**6**; $\text{R}^1 = (\text{CH}_2)_2-(\text{C}_6\text{H}_4)$), $[(\eta^1\text{-CpSn})_4\text{S}_6]$ (**7**), and $[(\text{CySn})_4\text{S}_6]$ (**8**), (Figure 5, top). Structure **5** is a crystalline compound, which could not be obtained as an amorphous powder. Hence, it showed SHG in accordance with the hypothesis mentioned above. The other compounds all show WLG, even if the π -electrons were not directly conjugated to the cluster core (**6**), not delocalized (**7**) or if π -electrons were not present in the organic substituent (**8**). Hence, the initial assumption of an aromatic substituent R to be required for WLG was refined, because a sufficiently electron-rich ligand, like an aliphatic ring system, seemed to be sufficient.

The influence of the chalcogen involved in the composition of the heteroadamantane-type cluster core was explored by synthesis of the corresponding selenide analogues, $[(\text{PhSn})_4\text{Se}_6]$ (**9**; same emission spectrum as found for **1**, λ_{max} red-shifted by < 0.1 eV), $[(\text{BnSn})_4\text{Se}_6]$ (**10**), $[(\text{R}^1\text{Sn})_4\text{Se}_6]$ (**11**), $[(\eta^1\text{-CpSn})_4\text{Se}_6]$ (**12**), and $[(\text{CySn})_4\text{Se}_6]$ (**13**), which were also investigated with respect to their emission properties (Figure 5).

Except for compound **10**, the changes of the resulting WLG were minor (Figure 5a–c). However, crystalline **10** (Figure 5d) also generated white-light – in contrast to its crystalline sulfide analogue **5**, which showed the expected SHG. This effect however, could be easily explained upon measurement of the melting temperature for both clusters, which is much lower in the case of **10**. The conclusion was thus that **10** melts under laser irradiation, which also leads to loss of order, and thus allows for WLG (Figure 5e).

The variation of the cluster core can also address the group 14 element T. Changing T in clusters of the type $[(\text{PhT})_4\text{S}_6]$ to Ge or Si affords the compounds $[(\text{PhGe})_4\text{S}_6]$ (**14**) and $[(\text{PhSi})_4\text{S}_6]$ (**15**). Compound **14** is amorphous and exhibits WLG with a minor shift in the spectrum (Figure 6). For reasons discussed below, the homologous silicon compound **15** is crystalline, and correspondingly shows SHG, as was expected.

In an attempt to understand how the substituents influence the optical response of the molecular clusters, two of the synthesized crystalline compounds with the same core

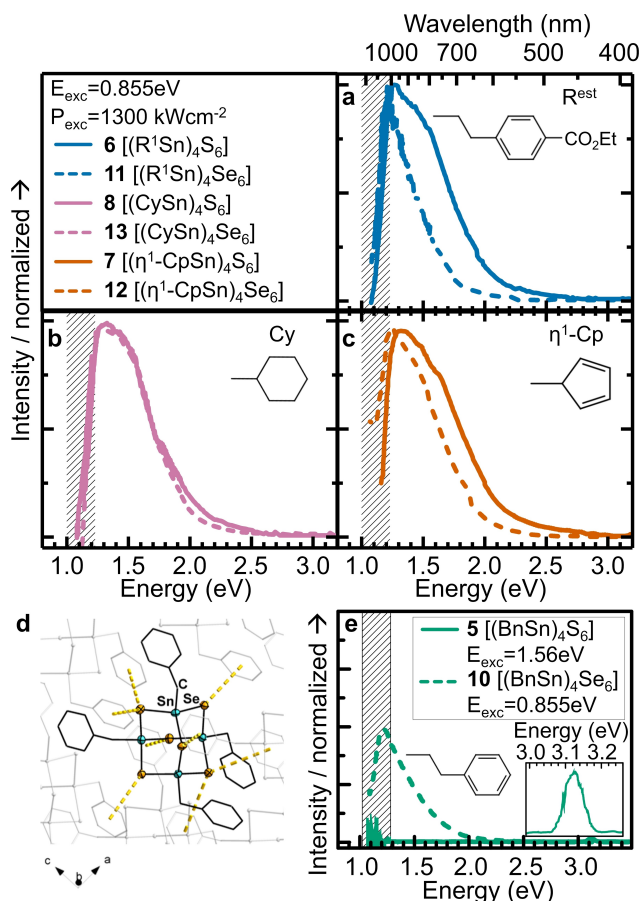


Figure 5. a–c: Emission spectra of the sulfide clusters **6**, **7**, **8** and emission spectra of the selenide clusters **11**, **12**, and **13** upon excitation with a 1450 nm (0.855 eV) laser. **d**: Cut-out of the crystal structure of compound **10**, as determined by single-crystal structure analysis. Emission spectra of **5** and **10** after excitation with a 1450 nm laser. **e**: The larger excitation wavelength was chosen in these experiments to suppress the excitation laser line. Reproduced under terms of the CC-BY license.^[10] Copyright 2019, The Authors, Published by Wiley-VCH.

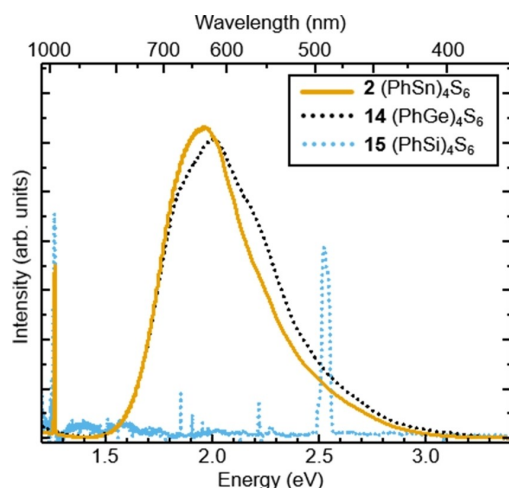


Figure 6. Emission spectra of **2**, **14**, and **15** after excitation with a 980 nm (1.265 eV) laser. Reproduced with permission from Ref. [12]. Copyright (2016) ACS.

but different substituents, **15** and the corresponding naphthyl compound, $[(\text{NpSi})_4\text{S}_6]$ (**16**), have been modeled within DFT utilizing periodic boundary conditions.^[9] Relaxed geometries as well as the HOMO and LUMO states for **15** and **16** are shown in Figure 7. While the substituents do not substantially influence the geometry of the molecular core, they have deep impact on the electronic structures and thus the optical response. The HOMO of **15** is localized on the cluster core, while the HOMO of **16** localizes on the naphthyl rings. The LUMOs of both systems are similar and localized on the substituents. Thus, the DFT-computed HOMO-LUMO gaps of the two systems are rather different and amount to 3.76 eV for **15** and 2.96 eV for **16**.

The calculated extinction coefficients of the two crystalline compounds are shown in Figure 8. The onset of the optical absorption corresponds exactly to the DFT-computed bandgap transition in the case of **16** (yellow dashed line), while it is at much higher energies in the case of **15** (blue dotted line). Indeed, the probability of a transition between valence band edge and conduction band edge is small, due to the different spatial localization and character of the two states.

The transitions leading to the absorption peaks of an individual cluster molecule are chiefly responsible for the major peaks in the dielectric function of the semiconducting crystals, suggesting that no new intermolecular low-energy electronic transitions occur when the molecules aggregate to form crystals. Thus, the deviations in the linear optical response of the two crystals originate from the qualitatively different and differently localized electronic states as determined by the ligands.

The calculation of the second-order polarizability tensor for the crystalline phases of **15** and **16** shows vanishing optical nonlinearities for all tensor components, as expected for a centrosymmetric crystal. Deviations from this behavior in experiments thus arise from structural defects and amorphous

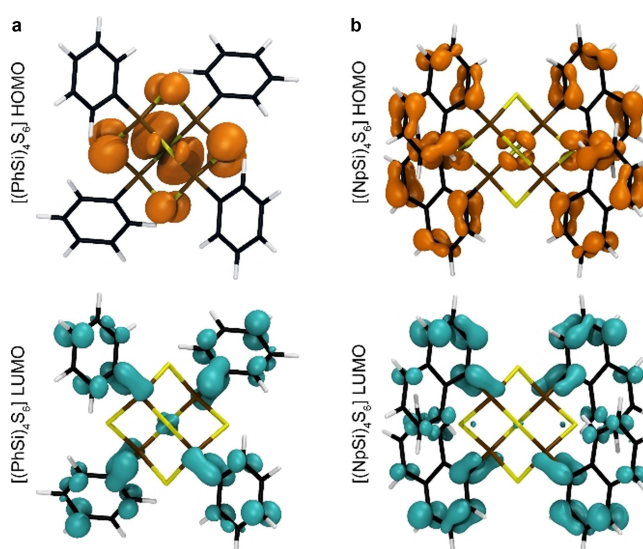


Figure 7. Optimized molecular structures and orbital characters of the HOMO and LUMO states of **15** (a) and **16** (b). Reproduced under terms of the CC-BY license.^[9] Copyright 2021, The Authors, Published by Wiley-VCH.

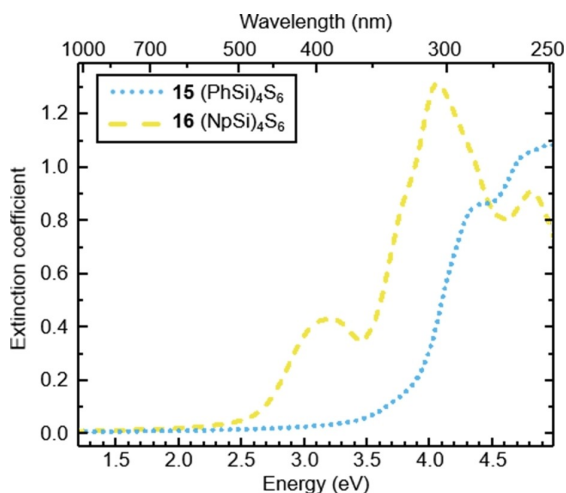


Figure 8. Extinction coefficient of molecular crystals calculated within the independent-particle-approximation (IPA) at the DFT equilibrium geometry, derived from either 15 (blue dotted line) or 16 (yellow dashed line). Reproduced under terms of the CC-BY license.^[9] Copyright 2021, The Authors, Published by Wiley-VCH.

regions in the samples as well as from surface-related contributions. At least for centrosymmetric crystals, they are not inherent bulk properties.

Another obvious change of the elemental composition of the core structure is observed with the purely organic compound adamantane, which actually serves as a patron saint of all of these clusters. Notably, the tetraphenyl derivative, 1,3,5,7-tetraphenyladamantane (17), can be obtained either in a crystalline or an amorphous habitus, dependent on the work-up procedure. Hence, it was possible to study not only the effect of another elemental composition, but to prominently prove the influence of the habitus on the nonlinear optical response. Indeed, single-crystals of compound 17 showed SHG, while an amorphous sample generated white light (Figure 9, left).^[13] Inspection of the power dependence of the WLG in 17 demonstrated that lower laser power shifts the spectrum to lower energies, as also found for 1. Furthermore, a weak SHG signal is detected at low pump energies (Figure 9, right).

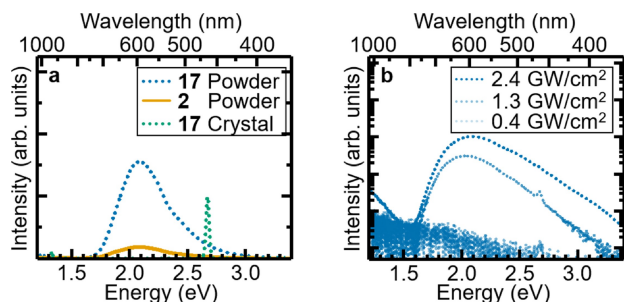


Figure 9. a: Emission spectra of crystalline as well as amorphous samples of compound 17 in comparison with the emission of compound 2, upon excitation with a 930 nm (1.333 eV) laser. b: Emission spectra of 17 upon excitation with a 930 nm laser at different pump powers. Reproduced with permission from Ref. [13]. Copyright (2018) Wiley-VCH.

In all systems with extreme nonlinear optical properties, second-harmonic generation is expected to be dominant at weak electrical field strengths. The fact that the transition was not observed in 1 at the investigated pump powers was explained by the lower band gap of the inorganic compounds relative to the organic structure, which leads to an enhancement of nonlinear optical effects by the fundamental transition dipole moment associated with the cluster core, as the detuning of the driving laser is smaller in this case.

As mentioned above, it remains unclear why homologous compounds tend to form amorphous powders or crystals – or both. A first step to construct a hypothesis was done with comprehensive theoretical work that considered molecular dimers as minimal models for extended systems.^[9] The DFT computations were performed on homologous clusters comprising different cluster cores and substituents, 2, 4, 15, and 16. All four cluster compounds are experimentally known: the organosilicon sulfide species are crystalline and the organotin sulfide clusters are amorphous, with obvious signs of beginning order according to the observation of SHG instead of WLG (see above). Figure 10 shows photographs of two of the solid materials, as used for the measurements of their emission properties.

The computations addressed possible relative orientations and the core-core distances that result in corresponding minimum energy structures with different numbers and geometric orientations of ligands facing each other. For Ph substituents, an “alternating dimer” arrangement of ligands opposing each other is slightly preferred on average, while for clusters with naphthyl substituents, a “stacked dimer” is slightly lower in energy. Figure 11 illustrates these two dimer structures, taking 15 as an example for the good agreement of the calculated model with the X-ray diffraction data.

The cluster dimers were explored with respect to their dissociation energies, which in addition were analyzed by decomposition of the binding energy into core-core interactions, core-substituent interactions, and substituent-substituent interactions. Some important conclusions can be drawn from these studies, the results of which are shown in Figure 12: First, Np substituents lead to stronger overall interactions than Ph substituents – in agreement with the assumption of beginning order in 4 that still appeared to be amorphous according to PXRD. Second, substituent-substituent interactions (blue color in Figure 12) are larger for R=Np than for R=Ph and core-substituent interactions (orange color in Figure 12) play a minor role only. Third, most unexpectedly but also most importantly, for T/E=Sn/S, core-core interactions (green color in Figure 12)

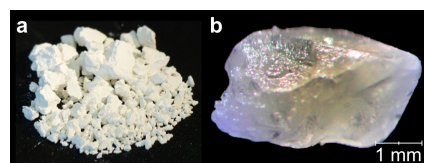


Figure 10. a: Photograph of a sample of 2 (amorphous powder). b: Photograph of a sample of 15 (single-crystal). Copyright (2016) ACS.

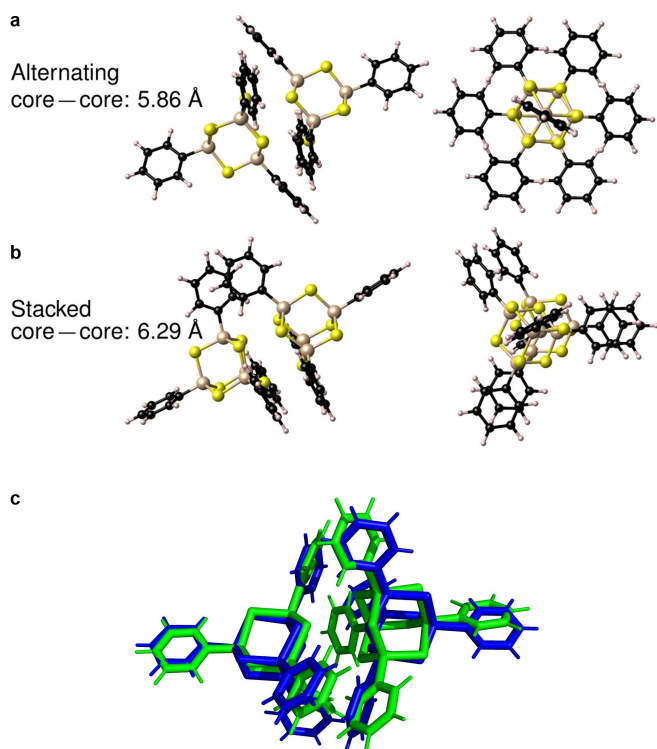


Figure 11. Calculated cluster dimers. **a:** Calculated dimer of **15** with alternating substituents (two views). **b:** Calculated dimer of **15** with stacked substituents (two views). **c:** Comparison of the relative orientation of two molecules of **15** as calculated (green, core-core distance 6.37 Å) and as found in the crystal structure (blue, core-core distance 7.05 Å),^[8] indicating good agreement of the model with the experimental data. Reproduced under terms of the CC-BY license.^[9] Copyright 2021, The Authors, Published by Wiley-VCH.

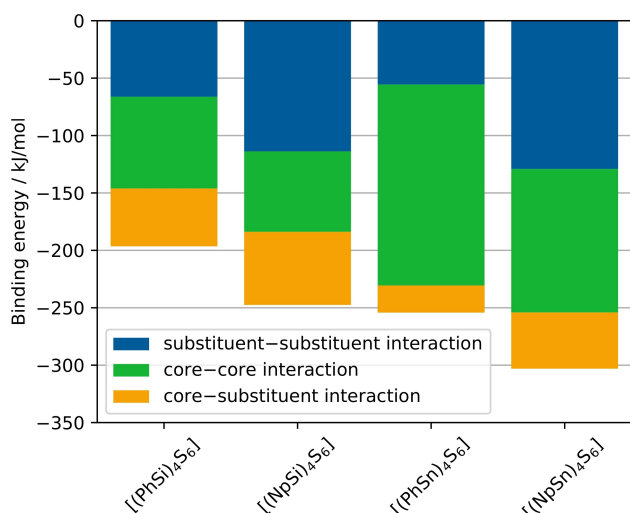


Figure 12. Calculated binding energies of dimers of the clusters in **15**, **16**, **2**, and **4** (from left to right), and specification of the decomposition of the energy into contributions from substituent-substituent, substituent-core, and core-core interactions. Reproduced under terms of the CC-BY license.^[9] Copyright 2021, The Authors, Published by Wiley-VCH.

are dominant (R=Ph) or equivalent to substituent-substituent interactions (R=Np) while for T/E=Si/S, substituent-substituent

interactions are dominant (R=Np) or equivalent to core-core interactions (R=Ph).

Thus, the higher tendency for crystallinity of the organo-silicon sulfide clusters in comparison with their tin analogs can thus be proposed to be attributed to the larger influence of the rather directional π -stacking interactions between the substituents. In contrast, the dominance of the comparably isotropic core-core interactions of the organotin sulfide clusters causes the intra-substituent effect on intermolecular order to fade into the background, which provides a possible explanation why this compound shows a distinctly lower tendency for order in the solid than the crystalline $[\text{Si}_4\text{S}_6]$ -based homologue. Molecule **4** appears to be the borderline case, as the two types of interactions are of similar strengths.

One of the remaining questions to date is the required regime of disorder for successful WLG. So far, it is clear that macroscopic disorder of the compounds, that is, the absence of long-range and (most probably) also medium-range order in amorphous or molten samples, is a sufficient condition for WLG to be caused by compounds of the type $[(\text{RT})_4\text{E}_6]$, given that the compounds possess substituents R that generally allow for WLG. As shown with the observation made for compound **4**, the order that already causes the compound to exhibit SHG can be below the radar of PXRD analyses. In order to explore whether disorder in the molecular regime would also be sufficient to cause WLG with a crystalline compound, we introduced perturbations to the molecular symmetry. This was done by replacement of T, E, or R with T', E', or R' in the cluster molecules. Many of such asymmetric adamantane-based compounds have been synthesized in the past, and some more are going to be reported soon. However, only one type of such compounds was investigated in terms of the emission properties, which will be presented here: By treatment of compound **2** with coinage metal phosphine complexes (formed in situ from $\text{MCl}:3\text{PMe}_3$ for $\text{M}=\text{Cu}, \text{Au}$ or $\text{AgCl}:3\text{PEt}_3$), it is possible to replace one Ph substituent with a metalloligand. The products $[(\text{Me}_3\text{P})_3\text{AuSn}](\text{PhSn})_3\text{S}_6$ (**18**), $[(\text{Et}_3\text{P})_3\text{AgSn}](\text{PhSn})_3\text{S}_6$ (**19**), and $[(\text{Me}_3\text{P})_3\text{CuSn}](\text{PhSn})_3\text{S}_6$ (**20**) were obtained as crystalline materials (see Figure 13).^[11]

According to the measurement of optical properties, the crystalline substances initially do not produce WLG. However, the crystals of compounds **18** and **19** apparently undergo a kind of amorphization during irradiation with the infrared laser, which was confirmed by PXRD and NMR experiments. As a

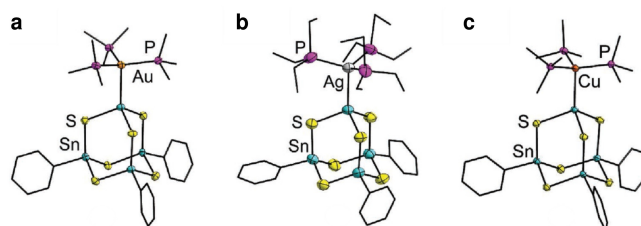


Figure 13. Molecular structures of **18** (a), **19** (b), and **20** (c). Organic substituents are shown as black wires with H atoms omitted for clarity. Reproduced with permission from Ref. [11]. Copyright (2019) Wiley-VCH.

result of this process, both compounds showed a WLG response very close to the original signal of **2**. Compound **20**, in contrast, did not show any emission under these conditions (Figure 14).

This was explained by a fundamentally different luminescence behavior of the copper compound: When comparing the photoluminescence response driven by a 266 nm laser of all three compounds, compounds **18** and **19** show a signal at about 2.84 eV, similarly to **2**, while **20** shows two discrete peaks at 1.45 and 2.34 eV. This allows re-absorption of photons in the visible spectrum, which effectively hinders WLG.

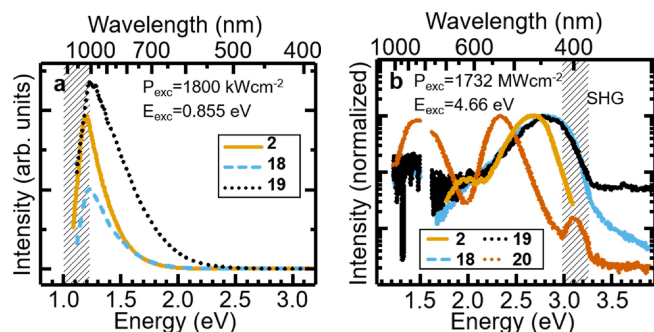


Figure 14. a: Emission spectra of compounds **2**, **18**, and **19**, indicating WLG upon irradiation with a 1450 nm (0.855 eV) CW laser. b: Photoluminescence response of **2**, **18**, **19**, and **20** after irradiation at 266 nm (4.66 eV). The missing data at 800 nm (1.55 eV) stems from the Ti:sapphire laser line which was frequency-tripled to achieve the 266 nm laser irradiation. The SHG at 400 nm (3.10 eV) is a side-effect of this procedure. Reproduced with permission from Ref. [11]. Copyright (2019) Wiley-VCH.

Table 2. Lowest triplet and singlet excitations [eV] calculated with TD-DFT for different density functionals with a cc-pVTZ(-PP) basis set.

Compound	State	BP86-D3	TPSS-D3	B3LYP-D3
18	Triplet	2.62	2.74	2.97
	Singlet	2.70	2.81	3.27
19	Triplet	2.82	2.94	3.33
	Singlet	2.91	3.03	3.50
20	Triplet	2.72	2.83	3.23
	Singlet	2.79	2.91	3.42

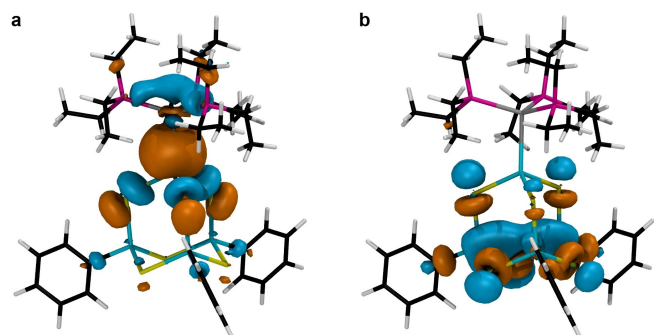


Figure 15. Orbitals of the lowest triplet (and singlet) excitation. The excitation takes place from the HOMO (a) to the LUMO (b). The orbitals are shown for the cluster **19** as an example [color code: Sn (turquoise), S (yellow), C (black), P (pink), H (white), and Ag (gray)]. Reproduced with permission from Ref. [11]. Copyright (2019) Wiley-VCH.

The experimental results are corroborated by quantum-mechanical atomistic calculations. Time-dependent density functional theory (TD-DFT) computations were performed with different functionals to estimate the lowest singlet and triplet excitations of the compounds **18**, **19**, and **20** (Table 2).

The calculated excitations increase slightly along $\text{Au} > \text{Cu} > \text{Ag}$. The lowest singlet excitation is in each case about 0.1 eV higher in energy. The orbitals relevant for the excitations are represented in Figure 15 exemplarily for compound **19**, as the HOMO and LUMO are very similar for the clusters **18**, **19**, and **20**. The HOMO exhibits σ_{AgSn} -like character with the main contribution from an Ag 5s orbital and small contributions of sulfur p-orbitals next to the complex, whereas the LUMO shows σ_{SnS}^* -like character at atoms most distant from the metal complex substituent.

Although the calculated excitation energies are very close to the experimental photoluminescence data (at least for compound **18** and **19**), a direct comparison is not possible, as Franck-Condon excitations are considered in our models. The deviation between the values calculated for **18** and **19** and the value calculated for **20** suggests more complex potential energy surfaces of the excited states and/or the ground states of the latter.

These first investigations of disorder on the molecular scale do not suggest that the presence of different ligands alone is a sufficient condition for WLG. However, many more studies need to follow, also addressing compounds with mixed inorganic-organic cluster cores, in order to investigate this aspect in more detail and to gain a comprehensive understanding of the required degree of disorder as a precondition of extreme nonlinear optical properties.

3. Conclusions and Outlook

Nonlinear optical properties have been observed for inorganic heteroadamantane-based compounds and for purely organic adamantane derivatives, one being strong SHG and the other one being a more extreme nonlinear effect that causes the generation of a supercontinuum, which in most cases covers the visible spectrum, and is therefore referred to as white-light generation (WLG). The two major prerequisites for such compounds to perform WLG as opposed to SHG are, first, an overall amorphous habitus and, second, the presence of an electron-rich organic substituent.

WLG apparently relies on a minimum degree of disorder in the solid state. So far, it could not be shown that an arbitrary arrangement of the molecules alone would be sufficient to cause WLG. Regarding the organic substituents, first ideas pointed to the requirement of delocalized π -electrons, which was in the meantime refined by the necessity of cyclic ligands including aliphatic cycles as substituents. It might be supposed that high electron density is needed in close proximity to the field gradient of the cluster core, leading to radiation emission by acceleration of the charge cloud. Properties of the emitted radiation depend inherently on the individual electronic and vibrational configuration.

Given that the two requirements mentioned above are met, fine-tuning of the emission properties can be realized by changing the organic substituents as well as the elemental composition of the cluster core. This, and the power of the exciting laser, allows to adopt the color-temperature of the emission to the one required for potential applications of the effect.

Research is ongoing as some important questions beyond which materials emit WLW remain unanswered to date. Is there a critical sample quantity, beyond which the effect can occur? Will a few molecular layers suffice and can nanoparticles scattered in a liquid equally cause the effect? Further aspects to be clarified are WLW efficiency, which materials are the most efficient ones in this regard, and the reasons for and controls of the unique directionality. In future work, it is also envisaged to polymerize the compounds or to embed them in a matrix while retaining their unique properties, which would be beneficial for processing and producing devices. The most obvious and most difficult question to answer, however, concerns the physical mechanism that causes the supercontinuum. This has not been clarified, and we expect that many more compounds need to be synthesized and investigated to gain a comprehensive picture of the processes during excitation and emission. Hence, we expect enormous research activity to emerge from these first studies that will ultimately lead to comprehension of the fascinating but as of now puzzling effect.

Acknowledgments

We express our gratitude for funding by the German Research Foundation (Deutsche Forschungsgemeinschaft, DFG) in the framework of the Research Unit FOR 2824. We are extremely thankful to Dr. N. Rinn and S. Schwan for their help with the manuscript. N. W. R. gratefully acknowledges funding from the Alexander von Humboldt Foundation within the Feodor Lynen Return Fellowship program. Open Access funding enabled and organized by Projekt DEAL.

Conflict of Interest

The authors declare no conflict of interest.

Keywords: adamantane-type clusters · chalcogenides · cluster compounds · inorganic-organic hybrid compounds · nonlinear optics · white-light generation

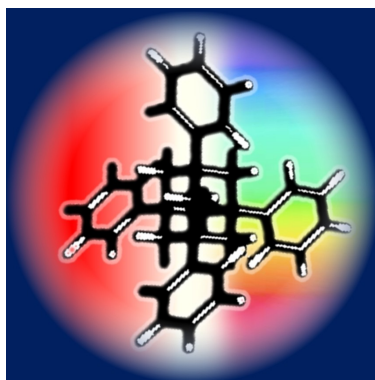
- [5] D. A. Akimov, M. Schmitt, R. Maksimenka, K. V. Dukel'skii, Y. N. Kondrat'ev, A. V. Khokhlov, V. S. Shevandin, W. Kiefer, A. M. Zheltikov, *Appl. Phys. B* **2003**, *77*, 299–305.
- [6] R. R. Alfano, *The Supercontinuum Laser Source: The Ultimate White Light*. Springer, Berlin, Heidelberg, **2016**.
- [7] J. Wu, G. Zheng, X. Liu, J. Qiu, *Chem. Soc. Rev.* **2020**, *49*, 3461–3483.
- [8] N. W. Rosemann, J. P. Eußner, A. Beyer, S. W. Koch, K. Volz, S. Dehnen, S. Chatterjee, *Science*. **2016**, *352*, 1301–1305.
- [9] K. Hanau, S. Schwan, M. R. Schäfer, M. J. Müller, C. Dues, N. Rinn, S. Sanna, S. Chatterjee, D. Mollenhauer, S. Dehnen, *Angew. Chem.* **2021**, *133*, 1196–1206; *Angew. Chem. Int. Ed.* **2021**, *60*, 1176–1186.
- [10] E. Dornsiepen, F. Dobener, S. Chatterjee, S. Dehnen, *Angew. Chem.* **2019**, *131*, 17197–17202; *Angew. Chem. Int. Ed.* **2019**, *58*, 17041–17046.
- [11] E. Dornsiepen, F. Dobener, N. Mengel, O. Lenchuk, C. Dues, S. Sanna, D. Mollenhauer, S. Chatterjee, S. Dehnen, *Adv. Opt. Mater.* **2019**, *7*, 1801793.
- [12] N. W. Rosemann, J. P. Eußner, E. Dornsiepen, S. Chatterjee, S. Dehnen, *J. Am. Chem. Soc.* **2016**, *138*, 16224–16227.
- [13] N. W. Rosemann, H. Locke, P. R. Schreiner, S. Chatterjee, *Adv. Opt. Mater.* **2018**, *6*, 1701162.
- [14] K. Merzweiler, H. Kraus, *Z. Naturforsch.* **1994**, *49b*, 621–626.
- [15] J. A. Forstner, E. L. Muetterties, *Inorg. Chem.* **1966**, *5*, 552–554.
- [16] D. Kobelt, E. F. Paulus, H. Scherer, *Acta Crystallogr. Sect. B* **1972**, *28*, 2323–2326.
- [17] R. H. Benno, C. J. Fritchie, *J. Chem. Soc. Dalton Trans.* **1973**, *422*, 543–546.
- [18] B. J. C. J. Bart, J. J. Daly, *J. Chem. Soc. Dalton Trans.* **1975**, *111*, 2063–2068.
- [19] A. Müller, W. Nolte, S. J. Cyvin, B. N. Cyvin, A. J. P. Alix, *Spectrochim. Acta* **1978**, *34 A*, 383–386.
- [20] A. Blecher, M. Dräger, B. Mathiasch, *Z. Naturforsch. B* **1981**, 1981.
- [21] D. Dakternieks, R. Edward, *Organometallics* **1993**, *12*, 2788–2793.
- [22] H. Berwe, A. Haas, *Chem. Ber.* **1987**, *120*, 1175–1182.
- [23] Z. Hassanzadeh Fard, L. Xiong, C. Müller, M. Holyńska, S. Dehnen, *Chem. Eur. J.* **2009**, *15*, 6595–6604.
- [24] A. Haas, H. J. Kutsch, C. Krüger, *Chem. Ber.* **1987**, *120*, 1045–1048.
- [25] I. Schellenberg, C. Pöhlker, R. Pöttgen, S. Dehnen, *Chem. Commun.* **2010**, *46*, 2605–2607.
- [26] Z. You, J. Bergunde, B. Gerke, R. Poettgen, S. Dehnen, *Inorg. Chem.* **2014**, *53*, 12512–12518.
- [27] D. Dakternieks, K. Jurkschat, H. Wu, E. R. T. Tiekink, *Organometallics* **1993**, *12*, 2788–2793.
- [28] T. Weidner, N. Ballav, U. Siemeling, D. Troegel, T. Walter, R. Tacke, D. G. Castner, M. Zharnikov, *J. Phys. Chem. C* **2009**, *113*, 19609–19617.
- [29] M. Gallant, M. Kobayashi, S. Latour, J. D. Wuest, *Organometallics* **1988**, *7*, 736–739.
- [30] C. Von Hänisch, M. Feierabend, *Z. Anorg. Allg. Chem.* **2013**, *639*, 788–793.
- [31] B. Zobel, M. Schürmann, K. Jurkschat, D. Dakternieks, A. Duthie, *Organometallics* **1998**, *17*, 4096–4104.
- [32] H. Newman, *Synthesis (Stuttg.)* **1972**, 692–693.
- [33] Z. Hassanzadeh Fard, C. Müller, T. Harmening, R. Pöttgen, S. Dehnen, *Angew. Chem.* **2009**, *121*, 4507–4511; *Angew. Chem. Int. Ed.* **2009**, *48*, 4441–4444.
- [34] I. Boldog, A. B. Lysenko, E. B. Rusanov, A. N. Chernega, K. V. Domasevitch, *Acta Crystallogr. Sect. C* **2009**, *65*, o248–o252.
- [35] R. L. McGreevy, L. Pusztai, *Mol. Simul.* **1988**, *1*, 359–367.
- [36] R. L. McGreevy, *J. Phys. Condens. Matter* **2001**, *13*, R877–R913.
- [37] O. Gereben, P. Jován, L. Temleitner, L. Pusztai, *J. Optoelectron. Adv. Mater.* **2007**, *9*, 3021–3027.
- [38] B. D. Klee, E. Dornsiepen, J. R. Ställhorn, B. Paulus, S. Hosokawa, S. Dehnen, W.-C. Pilgrim, *Phys. Status Solidi B* **2018**, *255*, 1800083.
- [39] B. D. Klee, B. Paulus, S. Hosokawa, M. T. Wharmby, E. Dornsiepen, S. Dehnen, W.-C. Pilgrim, *J. Phys. Commun.* **2020**, *4*, 035004.

- [1] S. Nakamura, T. Mukai, M. Senoh, *Appl. Phys. Lett.* **1994**, *64*, 1687.
- [2] S. Nakamura, *Rev. Mod. Phys.* **2015**, *87*, 1139.
- [3] C. Poriel, J. Rault-Berthelot, *Adv. Funct. Mater.* **2020**, *30*, 1910040.
- [4] T. Jiang, Y. Liu, Z. Ren, S. Yan, *Polym. Chem.* **2020**, *11*, 1555–1571.

Manuscript received: June 14, 2021
 Revised manuscript received: August 10, 2021
 Accepted manuscript online: August 18, 2021
 Version of record online:  

MINIREVIEWS

White-light generation: This Minireview summarizes current developments in the field of supercontinuum generation with amorphous molecular materials. The compounds in the focus of this work share a common general formula, $[(RT)_4E_6]$ ($T = C, Si, Ge, Sn$; $E = CH_2, S, Se, Te$), in which a molecular organic or inorganic adamantane-shaped cage is surrounded by four organic ligands R. All substances investigated in this context are described along with the results of experimental and theoretical analyses of their optical properties and the key parameters that influence the supercontinuum generation.



Prof. Dr. S. Dehnen, Prof. Dr. P. R. Schreiner*, Prof. Dr. S. Chatterjee, Prof. Dr. K. Volz, Dr. N. W. Rosemann, Prof. Dr. W.-C. Pilgrim, Prof. Dr. D. Mollenhauer, Prof. Dr. S. Sanna*

1 – 10

Amorphous Molecular Materials for Directed Supercontinuum Generation

